ORIGINAL PAPER

Valérie Bertagna · René Erre · François Rouelle
Didier Lévy · Sébastien Petitdidier · Marius Chemla

Electrochemical impedance spectroscopy as a probe for wet chemical silicon oxide characterization

Abstract The kinetics of the chemical growth of silicon oxide in H_2O_2-containing ammonia solutions and its break-up by dilute ammonia solutions was investigated using electrochemical techniques and more specifically electrochemical impedance spectroscopy. The recording of the open circuit potential (OCP), complemented by successive impedance diagrams, demonstrates clearly the build-up of a silicon oxide passivating layer when hydrophobic Si surfaces are immersed in $NH_3 + H_2O_2$ solutions. The thickening of the chemical oxide coating mainly results in the decrease of the capacitance value together with the enhancement of the ohmic surface resistance. On the other hand, pure ammonia dilute solutions lead to the progressive destruction of this hydrophilic passivating surface oxide, which is revealed by the simultaneous decay of the real component of the impedance. Finally, we observed the break-up of the passive layer, characterized by a sudden drop of the OCP to a value quite identical to that obtained with a bare Si surface. This process resulted in a dramatic corrosion of the substrate surface.

Keywords Silicon · Surface oxide · Electrochemical impedance · Passivation

Introduction

An important step of semiconductor processing is the gate dielectric build-up on the silicon surface in the production of smaller and faster logic and memory devices. Advanced gate dielectric coatings, only a few atomic layers in thickness, are required in the new chip generation. For example, oxide thickness down to 20 Å or less for future integrated circuits was projected, with a possible reduction of destructive fails. In this respect, wet chemical processes included in the RCA cleaning method are more than ever under investigation [1, 2]. In this process, the ammonia/hydrogen peroxide mixture standard clean SC1 solution [3] is still extensively used to clean the silicon surface from particle contamination and to grow a new protecting silicon oxide layer, 0.6–2 nm thick, after the DHF (dilute HF solution) cleaning process. Research on the mechanism of oxide generation by this ammonia/hydrogen peroxide solution is still extremely active [4, 5], aiming at the optimization of the treatment parameters. The quality of this wet oxide is strongly dependent on the applied chemistry, and could be better when used with an ultrapure water/ozone mixture [6], because of a higher homogeneity and density [7]. Wet chemically grown oxides are hydrophilic, as a consequence of their surface Si-OH (silanol) groups. A mechanistic study of their growth on n-type Si and their subsequent dissolution in ammonia was studied at 70 °C by van den Meerakker et al. [8]. More recently, the structure of these oxides was examined by scanning tunneling microscopy and shown to be constituted of islands, whereas oxides formed in the gas phase were uniform [9].

In this study, we examine in situ the growth rate of a passivating oxide layer on p-type Si samples immersed in a dilute ammonia solution containing hydrogen peroxide (APM), using electrochemical methods such as open circuit potential (OCP) measurements and electrochemical impedance spectroscopy (EIS) under zero current potential. In a previous publication [10], the variation of the OCP was shown to be a very sensitive parameter reflecting the reactivity of a silicon surface in various etching solutions. On the other hand, AC impedance measurements were used for the characterization of Si oxides grown by anodic polarization in a NH_4OH

V. Bertagna (✉) · R. Erre
Centre de Recherche sur la Matière Divisée,
CRMD, Université d'Orléans, Rue de Chartres,
B.P. 6759, 45067 Orléans, France
E-mail: mchemla@ccr.jussieu.fr

D. Lévy · S. Petitdidier
STMicroelectronics, 38926 Crolles, France

F. Rouelle · M. Chemla
Laboratoire d'électrochimie LI2C, Université P. & M. Curie,
4 Place Jussieu, 75005 Paris, France

electrolyte [11] at different voltage values under a steady-state current density, reaching a few mA/cm^2. In our experiments the EIS technique was applied at zero current potential in order to prevent any change of the oxide layer during the measurement. In this condition the constant phase element (CPE) modeling the impedance loop was identified by an almost ideal RC circuit. The same techniques were useful to prove the break-up of this hydrophilic protecting layer by a pure ammonia dilute solution.

Fig. 1 Simple equivalent circuit of the Si/electrolyte interface. *Rs*: series resistance (electrolyte and leads); *Rsc* and *Csc*: resistance and capacitance of the semiconductor depletion layer; *Rct* and *Cdl*: charge transfer resistance and capacitance of the double layer interface

Experimental

The experiments were carried out on p-type silicon wafers (boron doped, 10^{15} at/cm^3), (100) oriented, 200 mm in diameter, purchased from MEMC Electronic Materials. The samples were mirror polished for MOS applications, and their back side covered with a Ga-In alloy. The electrochemical experiments were done in a special cell constructed in our laboratory. Although the characteristics of this cell were previously described [12], it seems worth to recall that it was designed to control several important parameters which may result in non-reproducible quantitative measurements. These parameters are mainly (1) the influence of light, (2) the dissolved oxygen in solution, and (3) the effect of confined electrolyte at the junction between the Si single crystal and the solution. The feeding device allows us to fill the cell under argon pressure with pre-degassed electrolyte, and to maintain it in an argon atmosphere. The electrolyte was connected to the reference electrode through a thin polypropylene bridge whose one end was, prior to the experiment, equilibrated with a solution identical with the working solution. This procedure prevented any contamination due to foreign species, mainly K$^+$ and Cl$^-$ ions. In the present work, all runs were performed in the dark, at room temperature generally equal to 25 °C. The area of the sample in contact with the electrolyte was 3 cm^2. Moreover, the solution was carefully deaerated by high-purity argon, N60 grade (l'Air Liquide), containing less than 0.1 ppm residual oxygen. The control of dissolved oxygen is important as indicated in our previous work, and confirmed by the careful study of Ogata et al. [13]. Degassing the ammonia solutions was carried out under isopiestic conditions, i.e. the argon gas was beforehand bubbled through a large volume of ammonia solution at the same concentration. The studied samples were either hydrophobic, the final treatment being a HF + HCl mixture during 20 min leading to a bare H-terminated surface, or hydrophilic, covered with an oxide layer a few angstrom thick, the final step being in SC1 reagent during 40 min, in the dark at room temperature. The solutions were prepared by using SLSI grade (sub-large-scale integration, metal elements below 1 ppb) reagents, and diluted with 18.2 MΩ ultrapure water (UPW) obtained after deionization and ultramicrofiltration (0.05 μm). The electrochemical parameters were determined with an EG&G PAR model 273A potentiostat connected to an impedance analyzer (Solartron 1260). A simplified equivalent circuit could be represented by three impedance components as shown in Fig. 1. The two loops due to the depletion layer and the Helmholtz layer respectively were observed in almost all experiments, but their relative magnitude was greatly potential dependent. In this study, the frequency range was selected so as to record the diagrams corresponding to the Si/solution interface, including the oxide layer capacitance and the charge transfer resistance. Generally, the frequency range was 40 Hz to 0.05 Hz, with a 10 mV signal amplitude, so that the time needed to obtain a spectrum was 2 min 21 s. This condition was also required for a limited variation of the oxide thickness during the data acquisition. Thus the repeatability of the Nyquist diagrams was quite suitable, provided the change of OCP during the data acquisition was slow. Most often, OCP for a few minutes and impedance plots were recorded alternately during the time of
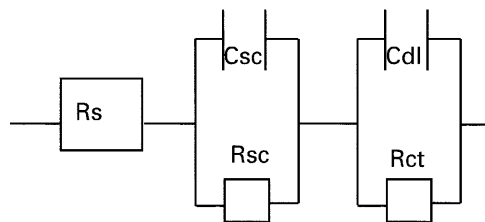
the experiment, thus establishing the correlations between time variations of OCP and EIS values.

Results and discussion

Open circuit potentials

We recall that OCP measurements proved quite useful to characterize the silicon surface anodic and cathodic site reactivity [14], and that they could be related to the surface chemistry reached by using FTIR, XPS, and ellipsometry [1].

The present results show that, when the Si surface is hydrophobic, i.e. not protected by a passive oxide layer, the OCP in oxidant-free ammonia is quite negative, near −1200 mV/SCE (Fig. 2a), indicating a high activity of the anodic sites in contact with NH$_3$ solution. This result is consistent with the observations of van den Meerakker et al. [8], who concluded that NH$_3$ molecules have a specific interaction with Si surface sites, since the corrosion rate in NH$_3$ is higher than in KOH solutions at the same pH. At the end of the experiment, the surface appeared rough and deeply corroded. Figure 2b shows
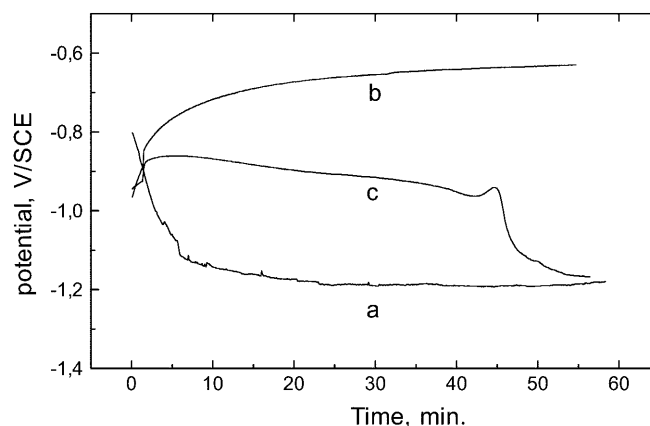

Fig. 2 Variation of the open circuit potential of p-Si, in the dark, as a function of time: *a* hydrophobic surface in a NH$_3$ solution; *b* hydrophobic surface in a NH$_3$ + H$_2$O$_2$ solution; *c* hydrophilic surface in a NH$_3$ solution

the OCP variation recorded as a function of time when the sample was first hydrophobic and the electrolyte solution was 1% NH_3 + 1% H_2O_2. The initial value of the potential was very negative (–950 mV/SCE), but, with time, the OCP moved towards more positive values to reach a plateau. Such behavior, related to a high activity of the cathodic sites, will result in the surface passivation process which is known to occur in the SC1 solution. At the end of the run, the surface was perfectly bright and became hydrophilic.

The same characterization method was also successful in following the surface reactivity of a hydrophilic surface in contact with a pure deaerated 1% NH_3 solution. The result is presented on Fig. 2c, where the potential becomes smoothly more negative with time, with a sudden potential drop, which reflects the break-up of the protective layer efficiency. Indeed, both the final value of the OCP and the voltammetric records were similar to those obtained with the "not protected" Si samples. This experiment was complemented with scanning electron microscopy (SEM). For example, during the first stage of Fig. 2c, when the OCP remained almost constant, the Si surface appeared bright and flat, although the protecting properties of the oxide were weakened, as indicated in the following EIS measurements. SEM observation could just detect a few circle-shaped defects, as shown in Fig. 3. These precursors of corrosion sites are quite similar to those described in Knotter's recent publication [4]. However, immediately after the steep drop of potential, a dramatically fast corrosion took place, so that within a few minutes the whole surface aspect became suddenly rough showing deep corrosion, with the appearance of micropyramids [15]. Figure 4 presents an example of these structures, which demonstrate the surface faceting along the (111)

crystal planes [16]. Of course, as soon as the very first corrosion pits are initiated, the wafer surface is damaged and will not be suitable for the fabrication of integrated circuits. It is worthy of note that the sudden drop of potential and the simultaneous surface degradation were obtained using thoroughly deaerated ammonia. In fact, in a complementary experiment using oxygen-saturated ammonia solution, OCP measurements were random and the formation of corrosion figures was much slower.

Electrochemical impedance spectroscopy

The results obtained with this method supported the assumption of the build-up, or alternatively the break-up, of the passive layer. They lead to the determination of quantitative parameters related to the changes of the surface reactivity. The measurements constituted a series of impedance diagrams inserted between the OCP monitoring plots. The range of frequencies was chosen so as to obtain the significant part of the diagram within a short time and thus have a constant surface condition during the data acquisition. Generally, a semiconductor interface is modeled by a simple equivalent circuit as proposed by Morrison [17], represented by two RC loops corresponding respectively to the space charge region and the Helmholtz layer, including the charge transfer reaction (Fig. 1).

The first example given in Fig. 5 represents the time variation of the Nyquist diagram resulting from the build-up of a passivating layer after reaction of NH_3 + H_2O_2 on an initially hydrophobic p-Si bare surface. This experiment corresponded to the procedure of Fig. 2b. The impedance plots, at zero current, are well-shaped semi-circles, the center being very close to the
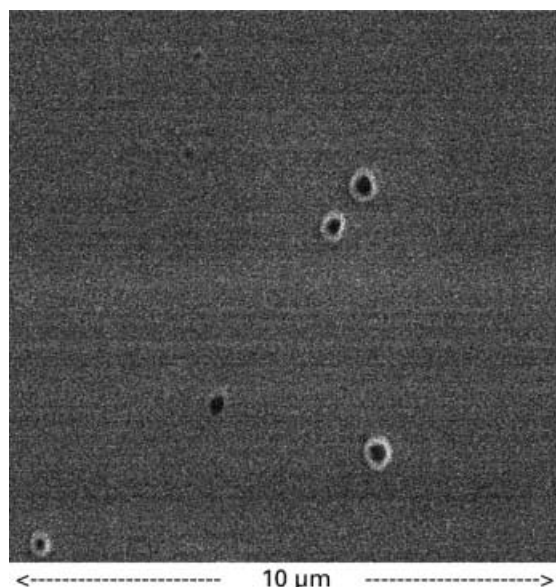

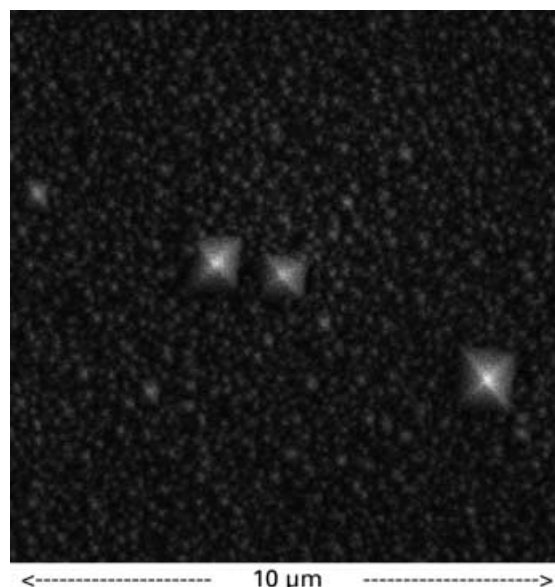**Fig. 3** Precursor corrosion figures on Si oxide layer in pure NH_3 deaerated solution

Fig. 4 Corrosion faceting with the formation of micropyramids on (100) p-Si in NH_3 deaerated solution
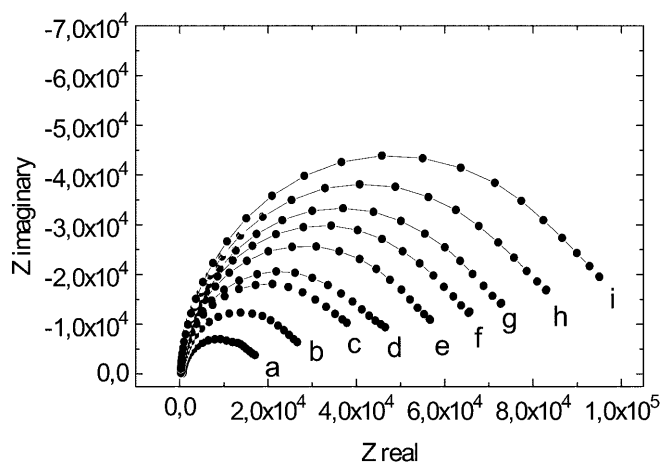
Fig. 5 Successive impedance diagrams of hydrophobic p-Si, in the dark, in a NH$_3$ + H$_2$O$_2$ solution; *a, b, c, d, e, f, g, h, i*: the diagrams are recorded at time intervals of 8 min

Fig. 6 Successive impedance diagrams of hydrophilic p-Si, in the dark, in a NH$_3$ solution; *a, b, c, d, e, f, g*: the diagrams are recorded at time intervals of 8 min

real axis, each corresponding to a simple RC equivalent circuit. Indeed, each set of numeric data was processed using the software from Boukamp [18] to obtain the constant phase element (CPE) representing the imaginary component of the interface. In fact it is known that oxide film/electrolyte interfaces exhibit a non-ideal capacitive behavior, and that a more accurate representation is obtained by substituting the capacitive component of the interfacial impedance $(i\omega C)^{-1}$, by a CPE equal to $Q(i\omega)^{-n}$, where $0 < n < 1$ is related to the phase angle φ equal to $n\pi/2$ [19]. In our experimental results, the data processing most generally lead to a CPE having a n parameter value very close to 1, typically 0.99, with a confidence factor χ^2 ranging between 10^{-3} and 10^{-4}. The adjustment thus corresponded to an almost pure capacitor of a few μF/cm^2. The diagrams show a steep increase of the polarization resistance from 5 to 30 10^4 Ω cm^2, while the capacity decreased from 4 to 1.5 μF/cm^2. It is interesting to note that a few voltammetric records in a narrow range of potential $\pm$50 mV near the OCP lead to the same value of polarization resistance. This fact, together with the capacitance properties, permitted the identification of the impedance loop as corresponding to the semiconductor/electrolyte interface in the frequency range studied here. This figure depicts the build-up of a passivating layer in NH$_3$ + H$_2$O$_2$, leading to a hydrophilic final bright surface, showing almost no defect with a scanning electron microscope. The capacitance decrease could be interpreted as a result of the oxide layer growth.

The opposite behavior was obtained with a hydrophilic p-type Si surface after SC1 treatment immersed in a pure deaerated dilute ammonia electrolyte. In this case, the diameter of the semi-circles strongly decreased with time (Fig. 6), indicating that the destruction of the protecting layer could be followed in situ. The experimental procedure corresponded to Fig. 2c of the OCP measurements. At the end of the experiment the Si surface appeared extremely rough due to a dramatic
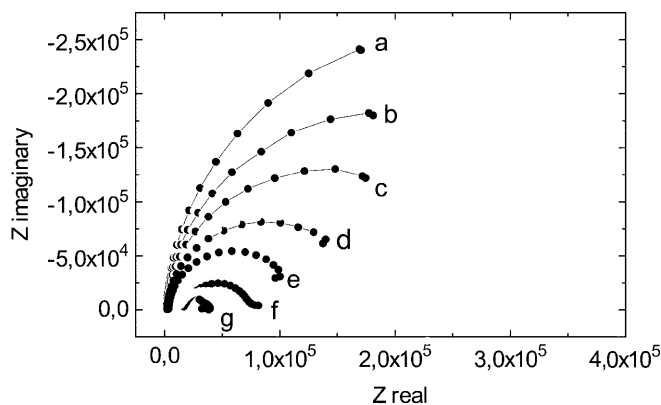
corrosion process resulting from the etching of the silicon substrate by the ammonia solution, leading to the appearance of (111) facets [20]. In fact, the observation of the surface by SEM showed the appearance of micropyramids (Fig. 4) as also obtained by Bressers et al. [21]. More generally, the electrochemical properties, OCP, EIS, and voltammetry, became similar to those obtained with a bare p-Si surface.

The influence of light was also investigated and revealed a deep change in the value of the impedance, as shown in Fig. 7. The overall value of the impedance, both in the resistance and capacitance contributions, was decreased 100-fold by illumination of the surface at 1400 lux intensity. This fact, already reported in a previous publication [22], is a direct consequence of the generation of charge carriers which induce an enhancement of the interface exchange current density and results in the silicon substrate photocorrosion [23]. It underlines the importance of controlling this parameter to reach quantitative data concerning semiconductors.

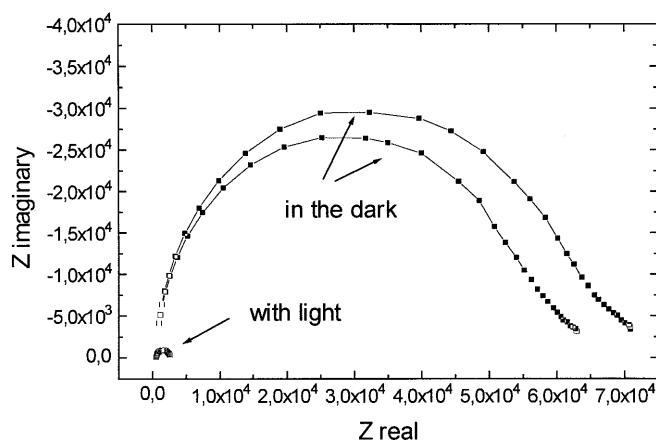To assign without ambiguity the recorded semi-circles to the components of the interfacial layers, preliminary

Fig. 7 Impedance diagrams of hydrophobic p-Si, in a NH$_3$ solution, in the dark, and illuminated with a 1400 lux intensity light

310

work has been undertaken in order to identify the contributions of the space charge region and the Helmholtz layer. This study was developed in acidic 0.1 M HCl dilute solutions because we observed that this condition was necessary to prevent the Si sample from corrosion and make the oxide layer stable in a rather wide range of bias potential. Detailed results of this study are out of the scope of the present publication. Thus it was easily possible to identify separately the circuits corresponding to (1) the silicon depletion layer with a capacitance near 0.01 μF, corresponding to the generally accepted value [11] from calculations using the Mott-Schottky equation and measurements of the flatband potential [11, 24], and (2) the oxide/electrolyte interface with a capacitance of a few microfarad, as indicated in previous publications [11, 24].

Moreover, we determined the charge transfer reaction rate by linear sweep voltammetry in a narrow range of potential ±50 mV near the OCP. We recall that the zero current at the OCP is the sum of anodic and cathodic currents. The exchange current is identical to the corrosion current, which is expressed as a function of the charge transfer resistance R_T:

$$i_{corr} = RT/(\alpha + \beta)FR_T \qquad (1)$$

where R is the ideal gas constant, T the temperature, F the Faraday constant, and α and β are the transfer coefficients which are determined by means of the voltammetric curves.

The slope of the curve at zero current $(dE/di)_{i=0}$ was used to determine the polarization resistance R_p, which was found to be equal to the values obtained from the diameter of the Nyquist plot, with a precision of about 5–10%. This argument was already advanced to deduce that this loop observed at low frequency represented the charge transfer reaction at the silicon/Helmholtz layer interface [24]. In our experiments, the measured polarization resistance R_p should include the charge transfer rate R_T plus the necessary ohmic drop through the wet oxide coating, which is permeable to ionic and molecular species.

A deep discussion for the derivation of quantitative data, capacitance and parallel resistance, from impedance measurements must start with the well-documented basic publication by Chazalviel [25], which describes several techniques of analysis. For simplification, in a rough approximation, the oxide layer could possibly be considered [11] as a compact insulator of area A, thickness d, and dielectric constant ϵ forming a capacitor:

$$C = f\varepsilon\varepsilon_0 A/d \qquad (2)$$

where f represents the surface roughness factor. Then the ratio $1/C$ should be proportional to the thickness d. Figure 8 represents the variation with time of the ratio $1/C$ in the situation where the oxide layer is growing, i.e. data from Fig. 5. The same approximation could also apply to the resistance in parallel to the CPE. In fact, the
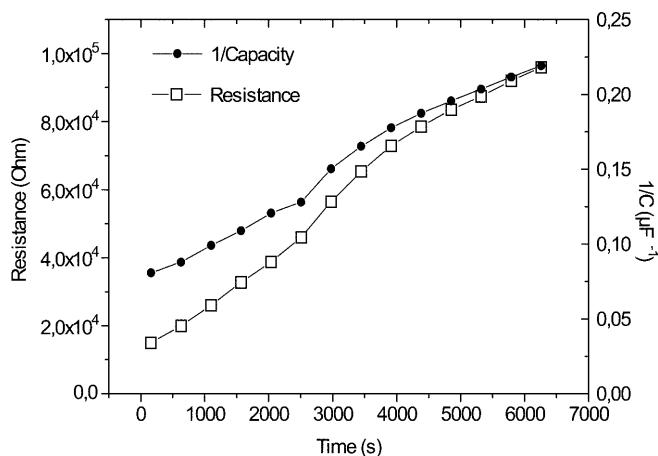

Fig. 8 Variation with time of $1/C$ and R values corresponding to the oxide growth in a $NH_3 + H_2O_2$ solution

electrical current between the Si surface and the electrolyte must undergo the ohmic drop through the oxide coating. The resistance could be written $R_p = \rho d/A$. Figure 8 shows a similar shape for R_p and $1/C$, indicating a roughly linear variation of the thickness versus time. A complementary measurement of oxide thickness was undertaken at ST Microelectronics R & D Center, using 200 mm p-Si wafers, after treatment with the same SC1 solution at room temperature. The final value of the oxide thickness, determined by a Optiprobe Thermowave 5220 ellipsometer, was found to range between 7 and 8 Å. Although we consider the model of the compact insulator as being oversimplified, we evaluated the expected value of the capacitance using Eq. 2, and the dielectric permittivity of SiO_2 passivating layers ($\epsilon = 3.8$) [26], and obtained a result of $C = 4.3 \ \mu F/cm^2$, which is rather close to the observed values.

As recalled in the recent paper by De Smedt et al. [27], growth kinetics, controlled by diffusion of the oxidizing species through the oxide layer to the interface, can be described by the Deal-Grove linear-parabolic equation [28]:

$$d^2 + Ad = B(t + \tau) \qquad (3)$$

where t is the oxidation time and τ a shift in the time axis, linked to the initial oxide layer already existing when measurements are started.

However, in ammonia solutions another term due to the dissolution rate of the oxide should be included. In the simplified mechanism, where the thickness growth is only controlled by diffusion of H_2O_2 in the oxide, and the dissolution rate is a constant per surface unit at constant ammonia concentration, the differential equation should be written as:
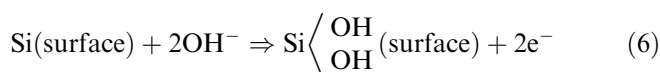
$$\partial d/\partial t = DC^\circ/d - k \qquad (4)$$

where D is the diffusion coefficient, C° is the hydrogen peroxide in solution, and k is the rate constant of oxide dissolution, this value being a constant for a given

concentration of NH_3. This equation shows that, at infinite time, d should reach a limiting value corresponding to the steady regime of the growth/dissolution process:

$$d = DC^{\circ}/k \qquad (5)$$

The shape of the curves in Fig. 8 shows that, in this experiment, the steady regime is not yet reached, the experiment being carried out at room temperature. In fact the experimental conditions seem to fit approximately the Deal-Grove model. However, the real process is much more complicated. Indeed, the wet Si oxide in alkaline ammonia solution shows a non-negligible permeability to water molecules and solute molecular and ionic species. This fact is proven by the observation by linear voltammetry [8] of a significant reduction current of H_2O_2 through the oxide layer, as well on p-Si as on n-Si samples.

In order to propose a mechanism of the growth and break-up of the passivating layer, the reaction of $NH_3 + H_2O_2$ solution on the Si surface was generally considered as a chemical reaction [8]. However, following Chen et al. [29], to treat the etching of Si at OCP as a purely chemical reaction with no electrochemical reaction involved is inappropriate. The existence of an exchange current is consistent with a contribution of an electrochemical mechanism, including an electron transfer between surface sites and the reactants in solution. In the case of SC1-like solutions, we can write:

$$Si(surface) + 2OH^- \Rightarrow Si\!\!\left\langle{OH \atop OH}\right. (surface) + 2e^- \qquad (6)$$

and:

$$H_2O_2 + 2e^- \Rightarrow 2OH^- \qquad (7)$$

Such a reaction will proceed by breaking the back bonds of the Si atoms and build-up of a passivating hydrated Si oxide growing on the Si lattice, while a following chemical reaction step leads to the dissolution of the oxide with the formation of a soluble silicate anion, through the overall chemical reaction [8]:

$$Si + 3OH^- \Rightarrow SiO_3^{2-} + 3/2H_2 + e^- \qquad (8)$$
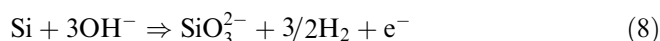
The set of chemical/electrochemical reactions 6, 7, 8 is consistent with the wet oxide on Si substrate growth/dissolution mechanism (Eq. 5).

However, when the solution contains only aqueous NH_3 species, evidently the dissolution process takes place in the same way as indicated here, making the oxide film thinner. However, injection of electrons will take place likewise through reaction 6. In the absence of oxidizing agent the cathodic reaction will concern only water molecules and result in H_2 evolution [8], and also the formation of Si-H bonds [24]:

$$2H_2O + 2e^- \Rightarrow H_2 + 2OH^- \qquad (9)$$

$$Si(surface) + H_2O + e^- \Rightarrow Si - H_{(surface)} + OH^- \qquad (10)$$
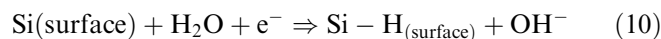
Such a mechanism, proposed by Cattarin et al. [24], leads to the formation of a hydrophobic Si-H layer at the interface with the Si oxide passivating layer, and contributes to loosen its protecting properties leading first to the appearance of a few corrosion pits as presented in Fig. 3, and followed by a rapid spreading of the process until the complete break-up of the passivation. The surface undergoes dramatic corrosion (Fig. 4), and its electrochemical properties become then identical to those of a bare Si substrate. This proposed mechanism suggests the following interpretation of R and C values presented in Fig. 9. The rapid decay of R is a result of the thinning down of the oxide film together with the appearance of a few corrosion pits. However, after the sudden drop of potential, the impedance of the outer Si/electrolyte interface being negligible, the measured impedance loop concerns the space charge region, the capacitance of which is near 10^{-8} F/cm^2. This peculiar behavior of p-Si explains the apparent increase of impedance observed in Fig. 9, and does not appear when the silicon substrate is n-type [30].

Conclusion

In the present study of chemical and electrochemical properties of the wet Si oxide generated in aqueous solutions, the measurements of OCP and EIS diagrams were obtained at room temperature, and showed the main characteristics of the oxide structure containing silanol groups. This loose structure shows a significant permeability to ions and H_2O_2 molecules which is necessary for the mechanism of oxide growth. A few complementary experiments, at temperatures ranging between 20 and 80 °C, using measurements obtained by ellipsometry, led to the conclusion that the limiting value of the oxide thickness was almost the same between 8 to 10 Å and nearly independent of the temperature, and then that the temperature variation of both parameters
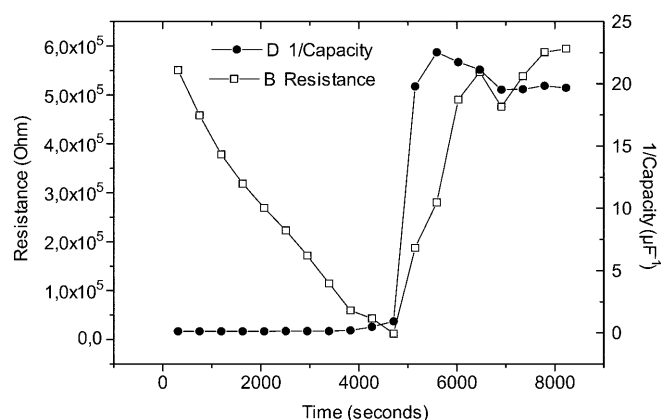

Fig. 9 Variation with time of $1/C$ and R corresponding to the destruction of the oxide layer in a deaerated NH_3 solution

312

D and k of Eq. 5 is almost identical. Summarizing the main results of this program, we can indicate that both aspects of this investigation, namely (1) the measurement of the surface layer electrical characteristics by electrochemical OCP and impedance spectroscopy and (2) the study of the fragility of the oxide protective properties by chemical reagents, constitute powerful tools for the characterization of surface chemical oxides and also for the new generation dielectric gate oxide a few monolayers thick. The electrochemical methods described in the present work will constitute a very convenient and efficient tool for a systematic study of the many parameters, such as the concentrations of the reactants, to optimize the thickness, the electrical properties, and the growth rate of the oxide.

References

1. De Smedt F, Vinckier C, Cornelissen I, De Gendt S, Meuris M, Gillis G, Heyns M (1999) Solid State Phenom 65–66:81
2. Kwalman LF, Geomini M, Levy D, Malgouyres D (1999) Solid State Phenom 65–66:31
3. De Gendt S, Knotter DM, Kenis K, Mertens PW, Heyns MM (1998) J Electrochem Soc 145:2589
4. Knotter DM, De Gendt S, Mertens PW, Heyns MM (2000) J Electrochem Soc 147:736
5. Celler GK, Barr DL, Rosamilla JM (2000) Electrochem Solid State Lett 3:47
6. Awaji N, Sugita Y, Ohkubo S, Nakanishi T, Takasaki K, Komiya S (1995) Jpn J Appl Phys 34:L1013
7. Sugita Y, Watanabe S, Awaji N (1996) Jpn J Appl Phys 35:5437
8. van den Meerakker JEAM, van den Straaten MHM (1990) J Electrochem Soc 137:1239
9. Aoyama T, Yamazaki T, Ito T (1996) J Electrochem Soc 143:2280
10. Bertagna V, Erre R, Rouelle F, Chemla M (1999) J Electrochem Soc 146:83
11. Schmuki P, Böhni H, Bardwell JA (1995) J Electrochem Soc 142:1705
12. Bertagna V, Rouelle F, Chemla M (1997) J Appl Electrochem 27:1179
13. Ogata YH, Ikeda T, Sakka T, Kobayashi T (2000) Electrochim Acta 45:2219
14. Bertagna V, Plougonven C, Rouelle F, Chemla M (1996) J Electrochem Soc 143:3532
15. Nojiri H, Uchiyama M (1992) Sens Actuators A 34:167
16. Allongue P (1996) Phys Rev Lett 77:1986
17. Morrison SR (1980) Electrochemistry at semiconductors and oxidized metal electrodes. Plenum Press, New York
18. Boukamp BA (1993) Equivalent circuit, version 4 51. University of Twente, The Netherlands
19. Gomes WP, Vanmaekelbergh D (1996) Electrochim Acta 41:967
20. Wang F, Shi Y, Liu J, Gu S, Zheng Y (1997) J Electrochem Soc 144:L37
21. Bressers PMMC, Kelly JJ, Gardeniers JGE, Elwenspoek M (1996) J Electrochem Soc 143:1744
22. Bertagna V, Rouelle F, Chemla M (1997) J Electroanal Chem 422:115
23. Levy-Clement C, Bastide S (1999) Z Phys Chem 212:123
24. Cattarin S, Musiani MM (1999) J Phys Chem B 103:3162
25. Chazalviel J-N (1990) Electrochim Acta 35:1545
26. Schultze JW, Lohrengel MM (2000) Electrochim Acta 45:2499
27. De Smedt F, Vinckier C, Cornelissen I, De Gendt S, Heyns M (2000) J Electrochem Soc 147:1124
28. Deal BE, Grove AS (1965) J Appl Phys 36:3770
29. Chen L-C, Chen M, Lien C, Wan C-C (1995) J Electrochem Soc 142:170
30. Bertagna V, Erre R, Rouelle F, Plougonven C, Chemla M (2000) In: Cleaning technology in semiconductor device manufacturing. (Electrochemical Society proceedings vol 99-36) Electrochemical Society, Pennington, NJ, pp 528–536